Deformable Templates for Tracking and Analysis of Intravascular Ultrasound Sequences*

Francisco Escolano, Miguel Cazorla, Domingo Gallardo and Ramón Rizo
Grupo i3a: Informática Industrial e Inteligencia Artificial
Departamento de Tecnología Informática y Computación
Universidad de Alicante
E-03690, San Vicente, Spain
Fax/Phone: 346-5903681
e-mail: sco@i3a.dtic.ua.es

December 2, 1997

Abstract

Deformable Template models are first applied to track the inner wall of coronary arteries in intravascular ultrasound sequences, mainly in the assistance to angioplasty surgery. A circular template is used for initializing an elliptical deformable model to track wall deformation when inflating a balloon placed at the tip of the catheter. We define a new energy function for driving the behavior of the template and we test its robustness both in real and synthetic images. Finally we introduce a framework for learning and recognizing spatio-temporal geometric constraints based on Principal Component Analysis (*eigenconstraints*).

1 Introduction

1.1 Intravascular Ultrasound Sequences

Intravascular Ultrasound is a recent technique which provides a source of high quality medical imaginery for precisely quantifying arterial obstruction and in consequence for the assessment of coronary interventions (bypass, balloon angioplasty, stent deployment or atherectomy) [27], [9]. A catheter with a transducer mounted on its tip is placed inside the artery and rotated to generate, by emitting pulses of ultrasound and receiving echoes, planar

*First International Workshop of Energy Minimization Methods in Computer Vision and Pattern Recognition, Venecia, Mayo, 1997. Lecture Notes in Computer Science.

cross-sections corresponding to the traversed arterial structure. In the output obtained (see Fig. 1) the center of the catheter is taken as origin of the new reference system and the image typically reveals three types of echo: *vessel lumen* (dark echoes), *plaque* (soft grey echoes) and *vessel wall* (white echoes). The analysis of the type of plaque helps specialists to choose the best interventional modality.

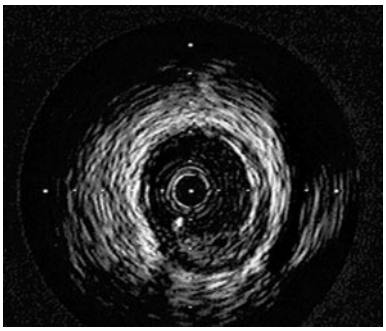

Figure 1: Slice obtained by intravascular ultrasound

1.2 Previous Approaches for Representation and Analysis

The problem of automatically obtaining suitable representations of the intravascular structure from two dimensional slices has been adressed in the past. These models must be suitable for extracting and analyzing quantitative features, in order to help both in diagnosis and intervention control. The most significant approaches developed to date are the following:

1. *Rendering Stacked Slices* [25], [17], [13], [23].
   (a) Static geometry and non-curved vascular structure are assumed. Visualizations are based on slice stacking. The problem of this approach is that the obtained geometry is usually unrealistic and distorted.
   (b) Extended approaches [19] introduce curved, but still static, structure.
2. *Introducing Snakes:* [12]
   (a) Spatio-temporal structure extraction by application of deformable models is addressed in the context of angiography (tracking of the 2D projections of the lumen).
   (b) Deformable models allow to obtain the actual dynamic geometry.
3. *Integration with Angiography:* [18]

(a) First step consists of obtaining, by variational stereo-matching based on snakes, the three-dimensional angiographic structure.

(b) This information is integrated, using the spatio-temporal synchronization of the transducer and the angiography, with the transversal slices for generating the visualization by volume rendering based on interpolation.

(c) In this sense slice positioning is guided by *landmarks* corresponding to branching points located at the arterial tree.

In our opinion future approaches must address the problem of analyze the internal structure of the slices in order to detect plaque (texture analysis) or to improve clinical procedures (e.g. angioplasty).

1.3 The Proposed Approach: Outline of the Paper

The approach presented in this paper is based on *Deformable Templates* [1], [10], [11], [15], [6], [28], [29], [30], [31], [20], [26]. In the context of intravascular ultrasound imaging we introduce improvements mainly in two directions:

1. *Wall Tracking:* given the morphology of the vessel walls (typically circular or elliptical), the problem of wall tracking can be addressed by using deformable templates. Wall tracking is interesting in, at least, two cases:

   (a) *Locating plaque:* once the wall is identified the zone where the plaque can be located is bounded . In consequence a texture driven local search, from the wall to the center of the vessel, can extract the actual boundary of the plaque in order to obtain the thickness of the lession. Tracking experiments with circular templates are presented in Section 2.2.

   (b) *Control of medical procedures:* In this context one of the medical procedures in which the use of non-rigid tracking can introduce some level of automation is the *Coronary Angioplasty*. Such procedure consists of placing a small baloon at the catheter end in order to dilate the plaque that obstructs the artery (see Figs. 2, 3 and 4). Balloon inflating induces a pressure that compresses and slashes the plaque and reduces or eliminates the arterial stenosis. In Section 2.3. we present several tracking experiments in angioplasty defining and using elliptical templates.

2. *Sequence Analysis:* given the spatio-temporal geometrical information derived from the application of the templates to the slices, it can be *learnt* and used for *recognizing* correct evolution paths in the angioplasty process (e.g. uniform expansion, unitary excentricity, etc.). We

propose the use of *Principal Component Analysis* in the temporal dimension for defining *compact spatio-temporal constraints*. In Section 3 we introduce this approach presenting several synthetic experiments.

Figure 2: Introduction of the catheter with a balloon.

Figure 3: Balloon deployment to compress and fracture the plaque.

Figure 4: Plaque extinction, stenosis clearing and flow normalization.

2 Tracking Based on Deformable Templates

A *single deformable template model* is defined by a *geometrical structure* $g_{\mathcal{D}}(\Theta)$ (circle, parabola, ellipse, segment, etc.), where Θ is a vector of relevant parameters and $\mathcal{D}$ is the spatial domain. This structure reacts to an specific *image model* or *potential field* $\Psi(u, v)$. Reaction behavior (dynamics) is established by an *energy function* $\mathcal{E}(\Theta)$. In this way optimal positioning of the structure over the potential is characterized by a minimum of $\mathcal{E}(\Theta)$ which is usually found by gradient descent. In this section we present the application of two types of templates (circular and elliptical) to track the inner wall of the artery.

2.1 Image Model: Potential Fields

As we need to bound the zone where the plaque can be we apply first grey thresholding. This is followed by a morphological closing which clears local structures that can introduce distortions, and, finally, we apply a Gaussian filter to smooth the geometry of the gradient. The result is showed in Fig. 5 whereas Fig. 6 contains the filtered gradient. Both images will be used as potential fields in our experiments.

This procedure gives us an ah-hoc *basic potential field* which contains the vessel wall. More robust fields can be obtained by applying a region

Figure 5: Binary potential fields after filtering.

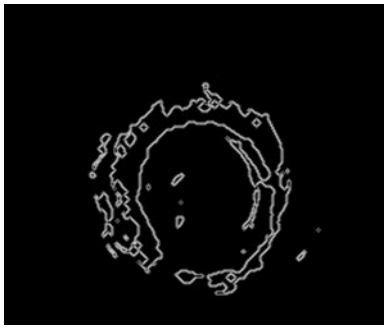

Figure 6: Gradient potential after Gaussian filtering.

Table 1: Circular Template Equations

Global Energy		
$\mathcal{E}(x,y,r)$	$\int\int_{\mathcal{D}} \mathcal{E}_{shape}(u,v,r) * \mathcal{E}_{image}(x+u,y+v)dudv + \mathcal{E}_{noise}(r)$	
$\mathcal{E}_{noise}(r)$	$\mathcal{E}_{image}(x,y)$	$\mathcal{E}_{shape}(x,y,r)$
$-\frac{\alpha}{a}r^a$	$\mathcal{I}(x,y)$	$(r-\sqrt{x^2+y^2})$
CT Dynamics		
Center Dynamics	$\begin{pmatrix} \frac{dx}{dt} \\ \frac{dy}{dt} \end{pmatrix} = -\begin{pmatrix} \frac{\partial \mathcal{E}}{\partial x} \\ \frac{\partial \mathcal{E}}{\partial y} \end{pmatrix} = \int_{\Gamma\cap\mathcal{D}}(r-\sqrt{u^2+v^2})(-\nabla\mathcal{I})ds$	
Radius Dynamics	$\frac{dr}{dt} = -\frac{\partial \mathcal{E}}{\partial r} = -\int\int_{\mathcal{D}} \mathcal{I}(x+u,y+v)dudv + \alpha r^{a-1}$	

based strategy [14], [24]. Moreover *speckle noise* or high correlated noise, due to the acquisition process and caused by tissue microstructures, can be modeled by a Rayleigh distribution [5].

2.2 Circular Templates: Wall Tracking and Initial Position

Circular Templates (CT) were first proposed in [32] as a part of a method to find the skeleton of a binary shape[1] with certain levels of noise tolerance. Let be (x,y) the center position, r the radius and $\mathcal{D}$ the circular domain bounded by the CT. We consider a binary image as potential: the function $I(x,y)$ returns 1 if the pixel is inside the template domain, and otherwise returns 0. The dynamic of the CT is defined by the function $\mathcal{E}(x,y,r)$, and its optimum is obtained by gradient descent. The original equations are showed at Table 1 and explained below:

[1] This model was originally named The Free-Travelling Circle.

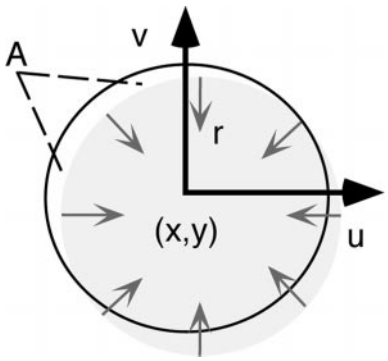

Figure 7: CT: Noise (A) and gradient forces

1. *Dynamics of the center:* Let be Γ the shape contour and ∇I the gradient. Then $-\nabla I$ can be considered as a force of opposite direction which is weighted by $r - \sqrt{u^2 + v^2}$. The CT motion will converge when all the forces inside the CT are balanced (See Fig. 7).

2. *Dynamics of the radius:* The first term is the white pixels area inside the CT domain (See area A in Fig. 7) and represents a force which makes the radius decrease. The second term is the expansion force of the CT. The CT will converge when the area A will be equal to αr^{a-1}. The α and a parameters determine the tolerated noise level. Tipical values used are: $1 < a < 3$ and $0 < \alpha < 20$.

We have applied this basic model to locate an estimate of the inner wall. The spatio-temporal structure obtained is showed, by rendering and interpolation, in Fig. 8. Arterial tightness can be observed at the bottom example. As we will see later, this approach is also useful to initialize other templates (like elliptical ones).

2.3 Elliptical Templates: Tracking in Angioplasty

As we said in the first section the shape geometry induced by inflating the balloon can be elliptical. In consequence we have extended the circular model to an elliptical one. Elliptical template formulation is given by the following terms (see Fig. 9):

1. *Geometrical structure, potential and global energy:* template elliptical structure is formulated by $g_{\mathcal{D}}(\Theta) = (x_c, y_c, a, b, \vec{V}_{ref})$ where: $\mathcal{D}$ is the elliptical domain, centered at (x_c, y_c), with major and minor axes a, b and with a reference vector $\vec{V}_{ref} = (\cos\theta, \sin\theta)$ being θ the orientation of the secondary axe (b). Using the potentials previously extracted, we derive the global energy:

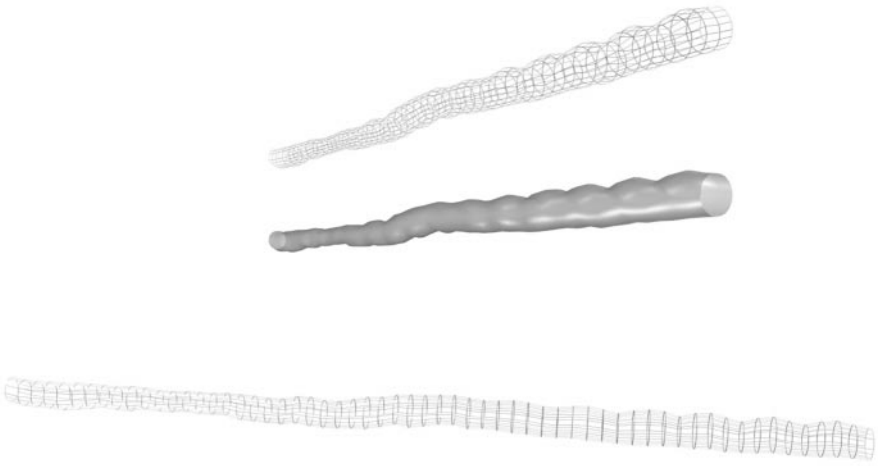

Figure 8: Rendered sequeces of inner radius.

$$\mathcal{E}(x_c, y_c, a, b, \vec{V}_{ref}) = \mathcal{E}_{shape}(x_c, y_c, a, b) + \mathcal{E}_{rot}(x_c, y_c, \vec{V}_{ref}) + \mathcal{E}_{noise}(a, b) \tag{1}$$

with the following terms:

(a) *Shape energy:* position, curvature and scale parameters are driven by:

$$\mathcal{E}_{shape}(x_c, y_c, a, b) = \iint_{\mathcal{D}} (1 - (\frac{u^2}{a^2} + \frac{v^2}{b^2}))\, \mathcal{I}(x_c + u, y_c + v)\, du\, dv \tag{2}$$

(b) *Rotation energy:* reference vector adapting behavior is based on:

$$\mathcal{E}_{rot}(x_c, y_c, \vec{V}_{ref}) = (\mathcal{N}(\vec{V}_{ref}) \cdot \mathcal{N}(\vec{\nabla}\mathcal{I}(p_1)))^2 \tag{3}$$

where $\mathcal{N}$ gives the unitary vector (in the direction of the argument), $\cdot$ represents the scalar product and p_1 is the first point of the positive semi-axe of a with nonzero gradient, that is:

$$p_1 = (x_c + i\cos(\theta - \frac{\pi}{2}), y_c + i\sin(\theta - \frac{\pi}{2})) \mid 0 < i < a, \vec{\nabla}\mathcal{I}(p_1) \neq 0 \tag{4}$$

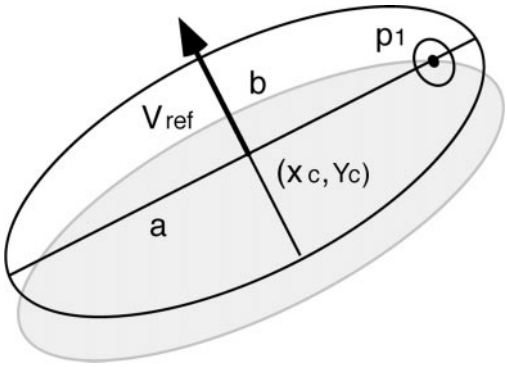

Figure 9: Elliptical Deformable Template.

(c) *Noise Energy:* the noise term allows to specify a different noise tolerance for each axe, and it is given by

$$\mathcal{E}_{noise}(a,b) = -\frac{\alpha_a}{\lambda_a}a^{\lambda_a} - \frac{\alpha_b}{\lambda_b}b^{\lambda_b} \tag{5}$$

2. *Dynamics of the ellipse:* the parameters that minimize $\mathcal{E}(x_c, y_c, a, b, \vec{V}_{ref})$ are obtained by gradient descent:

   (a) *Dynamics of the center :* similarly to the circular template, the dynamics of the center is given by the contact between the elliptical primitive and the gradient of the shape (vascular boundary):

$$\begin{pmatrix} \frac{\partial x_c}{\partial t} \\ \frac{\partial y_c}{\partial t} \end{pmatrix} = -\begin{pmatrix} \frac{\partial \mathcal{E}}{\partial x_c} \\ \frac{\partial \mathcal{E}}{\partial y_c} \end{pmatrix} = \int_{\mathcal{D}} (1 - (\frac{u^2}{a^2} + \frac{v^2}{b^2}))(-\vec{\nabla}\mathcal{I})ds -$$

$$2(\mathcal{N}(\vec{V}_{ref}) \cdot \mathcal{N}(\vec{\nabla}\mathcal{I}(p_1)))(\mathcal{N}(\vec{V}_{ref})\mathcal{N}(\vec{\nabla}^2\mathcal{I}(p_1))) \tag{6}$$

   The effect of the gradient is used to center the primitive (first term) and the point p_1 (second term). The second term has a secondary effect while the reference vector is not orthogonal to the gradient in p_1 or to its variation around this point (Laplacian), which is the equilibrium condition.

   (b) *Rotation Dynamics:* since the primitive could not be correctly oriented, a term to induce a rotation, when needed, must be introduced. For that reason we use the square of the dot product between the reference vector and the gradient vector at p_1. This gives us an estimate of the deviation with respect to the ideal orientation (orthogonal):

$$\begin{pmatrix} \frac{\partial \vec{V}_{ref_x}}{\partial t} \\ \frac{\partial \vec{V}_{ref_y}}{\partial t} \end{pmatrix} = - \begin{pmatrix} \frac{\partial \mathcal{E}}{\partial \vec{V}_{ref_x}} \\ \frac{\partial \mathcal{E}}{\partial \vec{V}_{ref_y}} \end{pmatrix} = -2(\mathcal{N}(\vec{V}_{ref}) \cdot \mathcal{N}(\vec{\nabla} \mathcal{I}(p_1)))\mathcal{N}(\vec{\nabla} \mathcal{I}(p_1))) \tag{7}$$

(c) *Dynamics of the axes:* the variation of the axes follows the same formulation that the circular model, and in each case is considered the noise factor associated to each axe:

$$\frac{da}{dt} = -\frac{\partial \mathcal{E}}{\partial a} = -\int\int_{\mathcal{D}} 2\,\frac{u^2}{a^3}\,\mathcal{I}(x_c + u, y_c + v)\,du\,dv + \alpha_a a^{\lambda_a - 1} \tag{8}$$

$$\frac{db}{dt} = -\frac{\partial \mathcal{E}}{\partial b} = -\int\int_{\mathcal{D}} 2\,\frac{v^2}{b^3}\,\mathcal{I}(x_c + u, y_c + v)\,du\,dv + \alpha_b b^{\lambda_b - 1} \tag{9}$$

the convergence will arrive when both noise levels be balanced by the number of included pixels.

Two examples of adaptation of the template are shown in Fig. 10. The left ellipse is one with a no elliptical shape. We fix the noise levels parameters in: $\alpha_a = 15$, $\alpha_b = 15$, $\lambda_a = 1$ and $\lambda_b = 1$. In the first case the adaptation deficience is due to the discrete nature of the rotation and to the no-elliptical shape, and in the second it is only due to discretitation errors.

Figure 10: Examples of Elliptical Templates.

We have found that, when using elliptical templates in a noisy environment, circular initialization improves the final result: the circular template is expanded in order to find the elliptical border and its radius and center position are used as the initial parameters for the elliptical template. This effect is showed in Fig. 11 and in Fig. 12. In Fig. 11, we present two sequences of experiments with increasing noise rate: in the upper sequence we have used elliptical initialization whereas at the bottom one we have used circles. The final results are better in the second case as we can corroborate in Fig. 12 where we represent, for each initialization policy, the Euclidean distance between the result and the actual shape for different levels of noise.

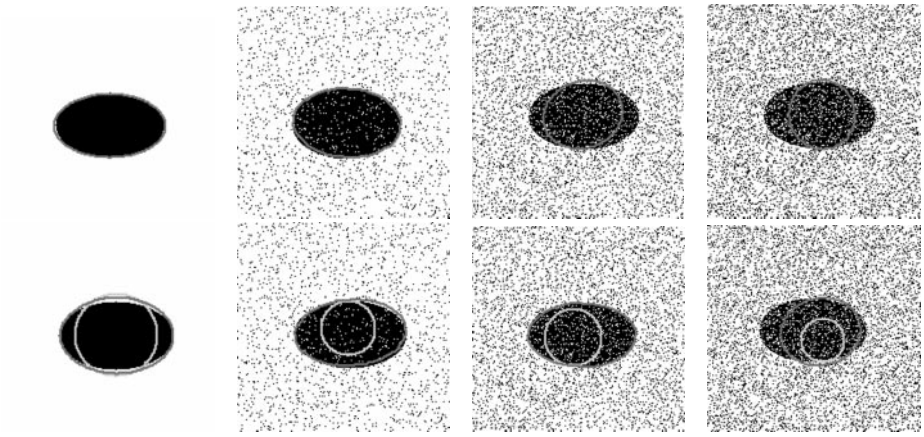

Figure 11: Analysis of noise tolerance. Effect of circle vs. elliptical initialization.

Final results of the aplication of the proposed model to an inflating sequence are shown in Fig. 13 where we can see some evolution steps. We have empirical selected the noise levels parameters as follows $\alpha_a = 4$, $\alpha_b = 5$, $\lambda_a = 2$ and $\lambda_b = 2$.

3 Spatio-Temporal Analysis: EigenConstraints

3.1 Motivation and Principal Component Analysis

Tracking of angioplasty based on deformable templates allows us to recover spatio-temporal data which can be very useful for experts (wall thickness, blood flow, etc.). In the Fig. 14 we can see the evolution of the inner radius. We can distinguish three stages. In the first one the radius decreases to reach a valley (frame number 11). This implies the existence of a lession. In the second stage (frames 14 to 30) we apply the balloon and the radius increases. Finally (third stage) at frame 30 we recover the normal behavior (oscillating peaks are related to cardiac pulse).

This fact motivates the development of representations for analyzing the evolution of the geometry along the sequence. In this sense we can design compact (low-dimensional) geometric constraints over interesting features or parameters obtained in the tracking process in order to define evolution cathegories. We address this question by using Principal Component Analysis (PCA) [8]. This method has been successfully applied to design deformable models [3], [4], [2] to learn and matching image models [21] and sequences [16], [22] and, finally, to represent primitive shapes [32].

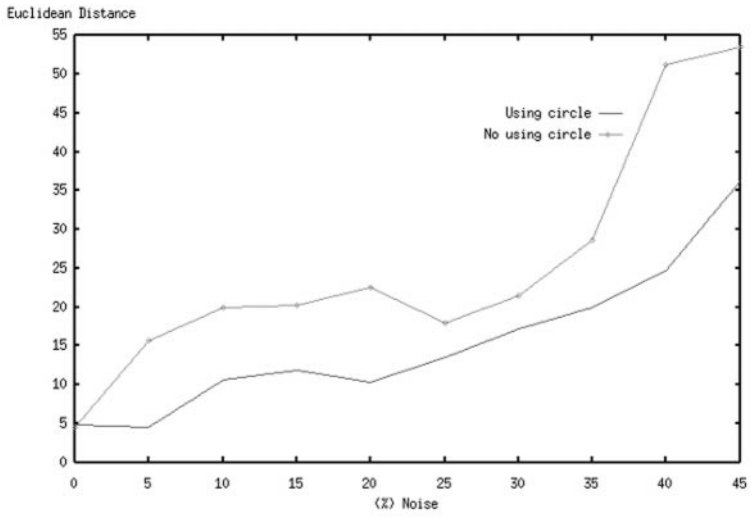

Figure 12: Initialisation behavior vs. increasing Gaussian noise levels.

3.2 Designing EigenConstraints

Given an spatio-temporal geometrical structure $\Theta(t)$ obtained by tracking we can define a set of constraints $C(t)$ which express *evolving geometric relations* (e.g. relative curvature between several parameters of $\Theta(t)$). The main purpose of using PCA in this context is to obtain a low-dimensional representation of the evolution of each relation over time.

As an illustrative example we have established three *ideal constraints* that must be satisfied by a correct inflating process: $r_a/r_0(t)$, $r_b/r_0(t)$, $r_a/r_b(t)$ (see Fig. 15). The two first relations express the local averaged evolution of each axe (local average is applied to filter cardiac pulses) normalized by the initial inner radius r_0, whereas the third express the relative evolution of the axes (i.e. an estimate of the excentricity) also locally averaged. Then it is preferred moderated (medium slope) and uniform (excentricity near the unit) balloon inflating. We have learnt these constraints and have expressed them with a reduced number of parameters (those corresponding to greater eigenvalues associated to the covariance matrix of the training set) to capture 90% of the variability. In Fig. 16 we represent acceptance results (by applying Mahalanobis distance [7]) for $r_a(t)/r_0$ given a prototype set of lines generated by varying their slope.

4 Conclusions and Future Developments

This paper first introduces the use of deformable templates for tracking the inner wall of vessels in intravascular ultrasound sequences. Tracking is

applied in two cases: a simple circular template is used to recover the inner wall along the transducer path and is also used for initializating an elliptical template for extracting wall shape evolution when inflating the balloon. In both cases exhaustive experiments where performed in order to find the ideal parameters of noise and to test the adequacy of each template to the problem. Finally a new framework based on eigenconstraints is presented for evolution recognition. The purpose of the later experiments is to show its potential application to the geometric analysis of the sequences. Future work includes: automatic learning of noise parameters, the improvement of the quality of the fields (e.g. solving boundary discontinuities) and, finally, extensive application of PCA to extract constraints to accurately define clinical quality criteria of the angioplasty process.

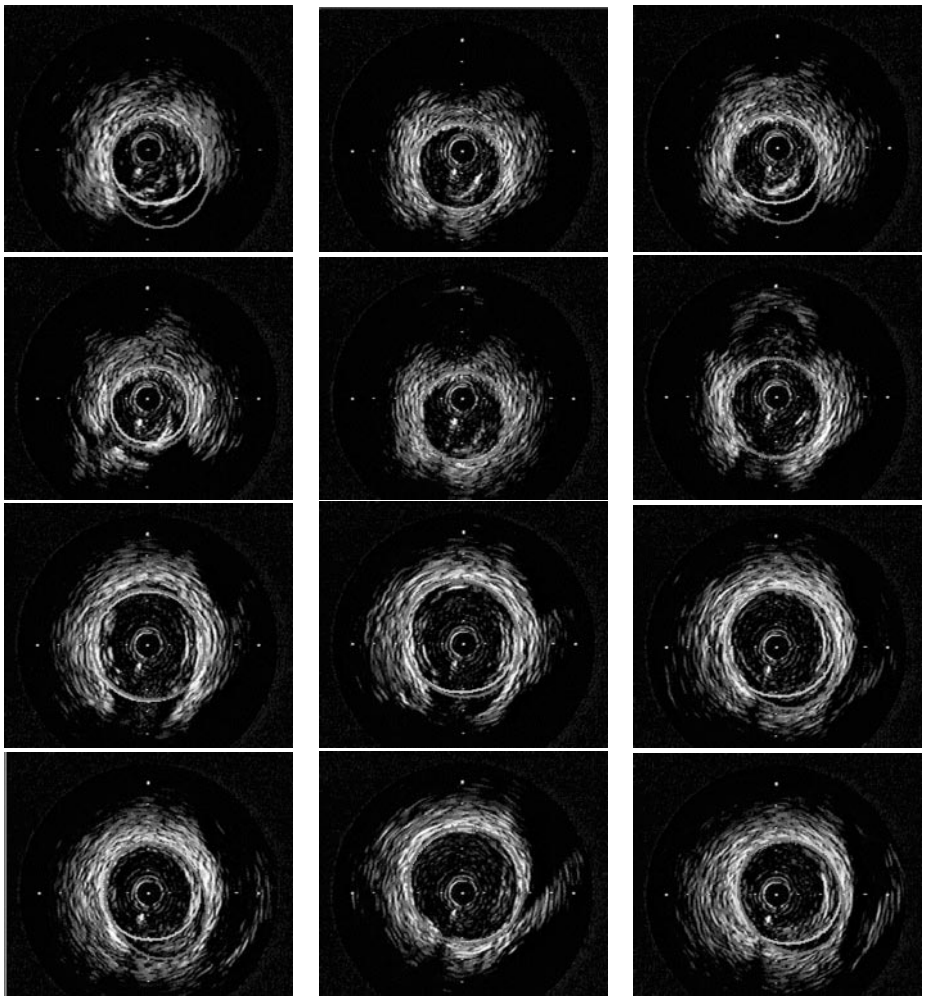

Figure 13: Tracking results in angioplasty.

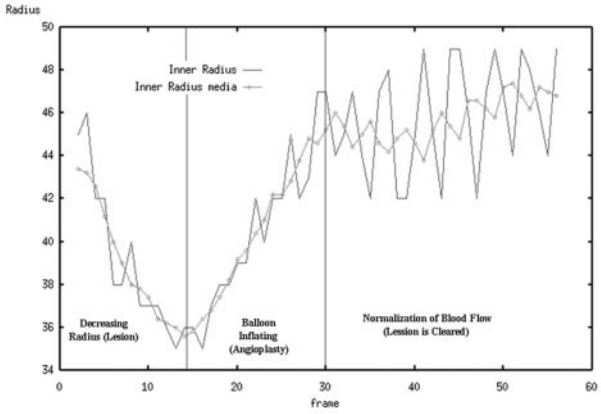

Figure 14: Evolution path of the inner radius.

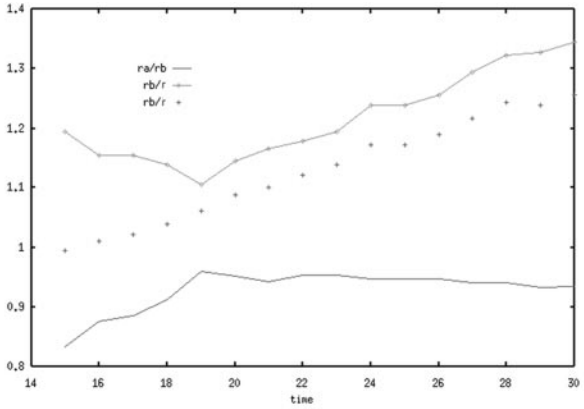

Figure 15: Ideal constraints for recognition.

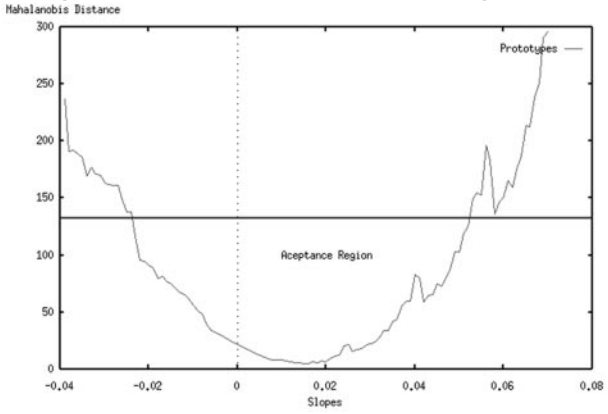

Figure 16: Experimental results for the $r_a/r_0(t)$ constraint. Prototype recognition.

References

[1] Amit, Y., Grenander, U., Piccioni, M.: Structural Image Restoration through Deformable Templates. J. Amer. Stat. Ass. **86** (1991) 376-387.

[2] Baumberg, A., Hogg, D.: Learning Flexible Models in Image Sequences. European Conference on Computer Vision. (1994)

[3] Cootes,T.F., Taylor, C.J., Cooper, D.H., Graham J.: Trainable Method of Parametric Shape. Image and Vision Computing. **10** (1992) 289-294

[4] Cootes, T.F., Taylor, C.J.: Active Shape Models. Smart Snakes. Proc. British Machine Vision Conference. (1992) 266-275

[5] Dias, J., Leytão, J.: Wall Position and Thickness Estimation from Sequences of Echocardiographic Images. IEEE Trans. Medical Imaging. **15** (1996) 25-38.

[6] Dubuisson, M., Lakshmanan, S., Jain, A.: Vehicle Segmentation and Classification Using Deformable Templates. IEEE Trans. PAMI. **18** (1996) 293-308

[7] Duda, R.O., Hart, P.E.: Pattern Classification and Scene Analysis. John Wiley and Sons. (1973)

[8] Fukunaga, K.: Introduction to Statistical Pattern Recognition. New York: Academic (1972)

[9] Goar, F. ST., Pinto, F.J., Alderman, E.L., Fitzgerald, P.J., Stadius, M.L., Popp, R.L.: Intracoronary Ultrasound Imaging of Angiographically Normal Coronary Arteries: An In Vivo Comparison with Quantitative Angiography. Journal of the American College of Cardiology. **18** (1992) 979-987

[10] Grenander, U.: General Pattern Theory: A Mathematical Study of Regular Structures. Oxford University Press. (1993)

[11] Grenander, U., Miller, M.: Representation of Knowledge in Complex Systems. J. Royal Stat. Soc. **56** (1994) 1-33

[12] Hyche, M., Ezquerra, N., Mullick, R.: Spatiotemporal Detection of Arterial Structure Using Active Contours. Proc. Visualization in Biomedical Computing. (1992) 52-62

[13] Isner, J.M., Rosenfield, K., Losordo, D.W., Krishnaswamy, C.",: Clinical Experience with Intravascular Ultrasound as an Adjunct to Percutaneous Revascularization. Intravascular Ultrasound Imaging. Ed. J.M. Tobis ,P.G. Yock. Churchill Livingstone Inc.,New York (1992) 186-197

[14] Ivins, J., Porril, J.: Active Region Models for Segmenting Medical Images. Proc. ICIP´94 (1994) 227-231

[15] Jain, A., Zhong, Y., Lakshmanan, S.: Object Matching Using Deformable Templates. IEEE Trans. PAMI. **18** (1996) 267-277

[16] Kirby, M., Weisser, F., Dangelmayr, G.: A model problem in the representation of digital image sequences. Patter Recognition. **26** (1993) 63-73

[17] Krishnaswamy, C., D'Adamo, A.J., Sehgal, C.M.: Three Dimensional Reconstruction of Intravascular Ultrasound Images. Intravascular Ultrasound Imaging. Ed. J.M. Tobis ,P.G. Yock. Churchill Livingstone Inc.,New York. (1992) 141-147

[18] Lengyel, J., Greenberg, D.P., Popp, R.: Time-Dependent Three Dimensional Intravascular Ultrasound. Proc. SIGGRAPH'95. (1995) 457-464

[19] Lengyel, J., Greenberg, D.P., Yeung, A., Alderman, E., Popp, R.: Three Dimensional Reconstruction and Volume Rendering of Intravascular Ultrasound Slices Imaged on a Curved Arterial Path. Proc. CVRMed'95. (1995)

[20] Lipson, P., Yuille, A.L., O´Keefe, D., Cavanaugh, J., Taafle, J., Rosenthal, D.: Deformable Templates for Feature Extraction from Medical Images. Proc. 1st European Conference on Computer Vision. (1990)

[21] Moghaddam, B., Pentland, A.: Face Recognition using View-Based and Modular Eigenspaces. M.I.T. Technical Report No. 301. (1994)

[22] Murase, H., Sakai, R.: Moving object recognition in eigenspace representation: gait analysis and lip reading. Patter Recognition Letters. **17** (1996) 155-162

[23] Roedlandt, J.R., Di Mario, C., Pandian, N.G., Wenguang, L., Keane, L., Slager, C.J., De Feyter, P.J., Serrius, P.W.: Three Dimensional Reconstruction of Intracoronary Ultrasound Images. Circulation. **90** (1994) 1044-1055

[24] Ronfard, R.: Region-Based Strategies for Active Contour Models. Int. Journal of Computer Vision. **13** (1994) 229-251

[25] Rosenfield, K., Losordo, D.W., Ramaswamy, K., Pastore, J.O., Langevin, E., Razvi, S., Kosowski, B.D., Isner, J.M.: Three Dimensional Reconstruction of Human Coronary and Peripheral Arteries from Images Recorded During Two-Dimensional Intravascular Ultrasound Examination. Circulation. **84** (1991) 1938-1956

[26] Xie, X., Sudhakar, R., Zhuang, H.: On Improving Eye Feature Extraction Using Deformable Templates. Pattern Recognition. **27** (1994) 791-799

[27] Yock, P., Linker, D., Angelson, A.: Intravascular Ultrasound: Technical Development and Initial Clinical Experience. Journal of the American Society of Echocardiography. **2** (1989) 296-304

[28] Yuille, A.L., Cohen, D.S., Halliman, P.W.: Feature Extraction from Faces Using Deformable Templates. Proc. CVPR. (1989) 104-109

[29] Yuille, A.L.: Generalized Deformable Models, Statistical Physics and Matching Problems. Neural Computation. **2** (1990) 1-24

[30] Yuille, A.L. Honda, K., Peterson, C.: Particle Tracking by Deformable Templates. Proc. International Joint Conference on Neural Networks. (1990)

[31] Yuille, A.L., Halliman, P.W.: Active Vision. Ed. A.L. Yuille ,A. Blake. MIT Press. (1992) 21-38

[32] Zhu, S.C., Yuille, A.L.: FORMS: A Flexible Object Recognition and Modelling System. Harvard Robotics Laboratory, TR No.94-1 (1994)